

## 650 9 Supplemental Materials

### 651 9.1 Roadway links and traffic activity

652 A detailed, link-based NO<sub>x</sub> emission inventory was compiled for roads in Detroit and surrounding Wayne  
653 County for the year 2010. NO<sub>x</sub> was selected as an air pollutant representative of emissions from traffic. A  
654 major part of this link-based emission inventory was the road network, including the locations of  
655 individual road links, link type based on the National Functional Classification (NFC), annual average  
656 daily traffic (AADT), and average speed information. These data were obtained for 9,701 road links that  
657 represent the study area (Figure 1). For the larger roads, e.g., major arterials and interstate highways,  
658 each traffic direction and/or group of lanes used separate links. All but local neighborhood streets and  
659 alleys were included in this network. AADT and speed data were derived using road counts and travel  
660 demand modeling (TDM) with link-specific inputs, e.g., AADT, number of lanes, roadway type and  
661 location, data provided by the Southeast Michigan Council of Governments (SEMCOG), the Michigan  
662 Department of Transportation (MDOT), and the US EPA Office of Transportation and Air Quality  
663 (OTAQ). The average speed for each link was estimated for four time periods: morning rush hour peak  
664 (7-9 AM), mid-day (9 AM – 3 PM), afternoon rush hour peak (3 PM – 6 PM), and off-peak (6 PM – 7  
665 AM).

666 Hourly traffic volume, fleet mix, and vehicle speed were estimated for each link as:

$$667 \quad V_{i,k,t} = FM_{NFC(i),k} MAF_{MON(t)} DAF_{k,DAY(t)} HAF_{NFC(i),t} AADT_i \quad (1)$$

668 where  $V_{i,k,t}$  (counts h<sup>-1</sup>) = number of vehicles on link  $i$  ( $i = 1 \dots 9701$ ) for vehicle class  $k$  ( $k = 1 \dots 8$ ) and  
669 hour of the year  $t$  ( $t = 1 \dots 8760$ );  $FM_{NFC(i),k}$  (dimensionless) = fleet mix allocation factor;  $MAF_{MON(t)}$   
670  $DAF_{k,DAY(t)}$ , and  $HAF_{NFC(i),t}$  are monthly, daily and hourly temporal allocations; and  $AADT_i$  = annual  
671 average daily flow. The 8 vehicle classes are aggregations from the MOVES emissions model that  
672 represent motorcycles, light-duty gasoline vehicles, light-duty diesel vehicles, light-duty gasoline trucks  
673 with gross vehicle weight (GVW) less than 6001 pounds, light-duty gasoline trucks with GVW > 6001  
674 pounds, light-duty diesel trucks, heavy-duty diesel trucks, heavy-duty gas vehicles, and heavy-duty diesel  
675 vehicles (MC, LDGV, LDDV, LDGT1, LDGT2, LDDT, HDGV, HDDV, respectively). These classes  
676 were derived using state-level data from the US Federal Highway Administration, and information from  
677 the US EPA Emission Inventory Improvement Program. NFC designations included classes 11, 12, 14,  
678 16, 17, 19 and 90, which represent interstates, other freeways, other principal arterials, minor arterials,  
679 major collectors, minor collectors and bridges, respectively.

680 The fleet mix allocation factor,  $FM_{NFC(i),k}$ , in eq. (1) gives the fraction of vehicles in vehicle class  $k$  for  
681 link  $i$ . This depends on the link's NFC designation, using allocation factors from Table VM-4 from the  
682 FHWA Highway Statistics Series (<http://www.fhwa.dot.gov/policyinformation/statistics/2010/vm4.cfm>)  
683 and information from the US EPA Emission Inventory Improvement Program  
684 (<http://www.epa.gov/ttn/chief/eiip/>). Summed across the 8 vehicle classes,  $\sum_{k=1 \dots 8} FM_{NFC(i),k} = 1$  for each  
685 road link. Only 3 short (<245 m) links were designated as NFC=90, for which NFC=11 was substituted,  
686 which had the highest fraction of diesel vehicles.

687 The temporal allocation factors account for variation in traffic flow by month, day of the week, and hour  
688 of the day. The monthly factor  $MAF_{MON(t)}$  ranged from 0.86 (December) to 1.10 (August), reflecting  
689 higher summer traffic. (Summed across the 12 months,  $\sum_{t=1 \dots 12} MAF_t = 12$ ). The day-of-week factor  
690  $DAF_{k,DAY(t)}$  portrayed slightly increased daily total volume for most vehicle classes on Friday (by 8%),  
691 and decreased volumes on Saturday (by 9%) and Sunday (21%), compared to other weekdays. Patterns  
692 for HDGV and HDDV classes differed: volumes were slightly lower flows on Friday (by 3%) and  
693 significantly lower on Saturday and Sunday (61 and 71%, respectively). (Summed across the 7 days in a  
694 week,  $\sum_{t=1 \dots 7} DAF_{k,DAY(t)} = 7$  for each vehicle class  $k$ .) The hour-of-day factor  $HAF_{NFC(i),HR(t),DT(t)}$  gave the  
695 diurnal pattern ( $HR(t) = 1 \dots 24$ ) for three day types (DTs, weekdays, Saturday, and Sunday), and was  
696 obtained from the SMOKE modeling system (<http://www.cmascenter.org/smoke/>). Generally, weekday  
697 patterns were bimodal with morning and afternoon rush hour peaks; weekends patterns were unimodal

698 with a broad afternoon peak, but patterns vary by road type as given by NFC. (Summed across the 24  
 699 hours in a day,  $\sum_{t=1..24} \text{HAF}_{\text{NFC}(i),\text{DT}(t),\text{HR}(t)} = 1$  for each NFC and DT.) For holidays, a Sunday schedule  
 700 was assumed ( $\text{DAF}_{k,\text{DAY}(t)}$  and  $\text{HAF}_{\text{NFC}(i),\text{HR}(t),\text{DT}(t)}$  were set to Sunday values). Holidays in year 2010 were  
 701 New Year's Day (Jan. 1), Memorial Day (May 31), Independence Day (July 5), Thanksgiving (Nov. 25),  
 702 and Christmas (Dec. 25). We confirmed that eq. (1) obtained the correct AADT by summing link  
 703 specific-flows over vehicle classes and hours of the year:

$$704 \quad \text{AADT}_i \approx 365^{-1} \sum_{k=1..8} \sum_{t=1,8760} V_{i,k,t} \quad (2)$$

705 Because AADT does not account for holidays, eq. (2) is not an equality, although differences are small.

## 706 **9.2 Emissions**

707 Hourly emissions were estimated for each of the 9,701 links as follows. First, emission factors for  
 708 primary exhaust emissions of each pollutant were calculated using MOVES2010a  
 709 (<http://www.epa.gov/otaq/models/moves/>), which uses a power-based approach that varies by vehicle  
 710 class, vehicle speed, ambient temperature, and fuel properties. Emission factors  $\text{EF}_{k,\text{SPEED},\text{TEMP},\text{MON}}$  (g  
 711  $\text{mile}^{-1} \text{vehicle}^{-1}$ ) were calculated for 8 vehicle class ( $k=1..8$ ), 16 vehicle speeds (2.5, 5, 10, 15 ... 75  
 712 mph), 11 ambient temperatures (0, 10, 20 ... 90, 100 °F), and 12 months (Jan. through Dec.) using  
 713 monthly average properties for fuels in the modeling domain, based on survey information from  
 714 SEMCOG. MOVES inputs were adjusted for the 2010 Detroit vehicle age distribution, based on an  
 715 analysis of vehicle registration information by the Lake Michigan Air Directors' Consortium (LADCO).  
 716 Emission factors from MOVES were applied to each road link to generate an hourly and link-based  
 717 emissions inventory that accounted for traffic activity, i.e., the volume of each vehicle class and the  
 718 average speed for each link and hour. Link-specific emission rates  $E_{i,t}$  ( $\text{g m}^{-1} \text{s}^{-1}$ ) for link  $i$  and hour  $t$  were  
 719 calculated as:

$$720 \quad E_{i,t} = 1.72604\text{E-}07 \sum_{k=1..8} \text{EF}_{k,\text{SPEED}(i,t),\text{TEMP}(t),\text{MON}(t)} V_{i,k,t} \quad (3)$$

721 where the first constant converts units of distance (1 mile/1609 m) and time (1 h/3600 s) to match the  
 722 vehicle counts and the MOVES emission factor units;  $\text{EF}_{k,\text{SPEED}(i,t),\text{TEMP}(t),\text{Month}(h)}$  is the emission factor (g  
 723  $\text{vehicle}^{-1} \text{mile}^{-1}$ ) from MOVES for link  $i$ , vehicle class  $k$ , link speed  $\text{SPEED}(i,t)$ , hourly average ambient  
 724 temperature  $\text{TEMP}(t)$ , and month  $\text{MON}(t)$ ; and  $V_{i,k,t}$  is the number of vehicles per hour for link  $i$ , vehicle  
 725 class  $k$ , and hour  $t$  given in eq. (1). Temperature and vehicle speed were placed into 11 and 16 bins,  
 726 described earlier, and lookup tables were used to select values. Temperatures were taken as the average  
 727 across five airport weather stations in the Detroit area, which yielded a complete and robust dataset.

## 728 **9.3 Dispersion Modeling**

729 Pollutant concentrations from vehicle emissions were predicted using RLINE  
 730 (<http://www.cmascenter.org/r-line/>), a research grade dispersion model for near-roadway assessments  
 731 under development by US EPA. This steady-state plume-dispersion model incorporates newly developed  
 732 algorithms for predicting concentrations from road sources, including at receptors very near roads and at  
 733 'upwind' receptors due to plume meandering. (Snyder, Venkatram et al. 2013, Venkatram, Snyder et al.  
 734 2013) RLINE utilizes numerical methods to integrate multiple point sources along a line source, or an  
 735 analytical approximation that provides similar results. Dispersion parameters were derived from field  
 736 data and recent wind tunnel experiments for near road sources. Hourly meteorological data were taken  
 737 from Detroit City airport, which was determined to be representative of the study area after examining  
 738 land use in the vicinity of the meteorological site, as well as correlations among surface measurements  
 739 obtained at this and four other area meteorological monitoring sites. These data were processed by  
 740 AERMET, which completed quality assessment checks, merged surface, upper air and on-site data, and  
 741 estimated boundary layer parameters.

742 Several sets of receptors were used. (Each receptor represents a discrete point or location.) The first used  
 743 extremely fine (10 m) resolution to model a high impact area, the intersection of I75 and I94. In this case,  
 744 12,221 receptors were laid out over a 1.0 x 1.2 km rectangular grid on 10 m centers (SW Universal

745 Transverse Mercator (UTM) coordinate of 330,000, 4,692,400). The second set used the same resolution  
746 to estimate concentrations in the vicinity of each of three NO<sub>x</sub> monitoring sites in the Detroit area (121  
747 receptors, 100 x 100 m area). The third modeled the entire Detroit area using 27,622 receptors over a  
748 34.5 x 23.0 km grid on 150 m centers (SW UTM coordinate of 311,500, 4,680,500). The SE corner of  
749 this region covering portions of the Detroit River, Lake St. Clair and Canada was excluded. In all cases,  
750 the modeled road network extended well beyond the receptor network.

#### 751 **9.4 Computational Considerations**

752 Estimating concentrations with high spatial resolution at the urban scale is computationally intensive. As  
753 an example, for the 9,701 road links, the 150 m grid spanning Detroit, and 8,760 hours per year, 2.34  
754 trillion source-receptor calculations are needed to determine annual average concentrations. This problem  
755 would require literally centuries for a standard workstation. Calculations were speeded up by using the  
756 analytical approximation in RLINE; estimating annual averages based on a subset of meteorology,  
757 specifically, every 6<sup>th</sup> day (found to provide representative results); revising the RLINE code to allow  
758 hourly emissions without post-processing; using look-up tables with precomputed emission profiles for  
759 each NFC and speed class combination; and breaking down receptors into several subsets that were run  
760 simultaneously on multiple computers. In addition, we considered only receptor-link distances less 25 km  
761 (roads at longer distances provide negligible impacts), and used an adaptive algorithm to further select  
762 link-receptor pairs based on distance and road link emissions. This algorithm was tailored to Detroit but  
763 is easily generalized. First, 1-hr concentrations were estimated for several "model" line sources (unitary  
764 emission rate, 20 and 2000 m long sources) using a radial receptor network (16 equally spaced "arms"  
765 with a logarithmic progression of distances and receptors from 10 m to 100 km from the source), RLINE,  
766 and 2010 Detroit meteorology. Then, the maximum annual average concentration at each distance was  
767 found and fitted to a simple model:

$$768 \quad C_x = 10^{[2.68346 - 1.45929 \log_{10}(x)]} \quad (4)$$

769 where  $C_x$  = fitted concentration at distance  $x$  (m), and the two coefficients are best fit parameters  
770 (calculated using linear regression on transformed variables). This model fitted the concentration  
771 envelope reasonably well ( $r=0.96$ ) and reflects a roughly logarithmic decay of concentrations with  
772 distance. For example,  $C_{x=20000m}$  is five orders of magnitude lower than  $C_{x=0m}$ . Next, the maximum  
773 possible near-field concentration for a high emitting source was calculated as the product of  $C_x$  with  $x=25$   
774 m, the highest hourly emission rate (over the year), and a relatively high volume link (AADT=100,000,  
775 NFC=11). Then, the potential impact of each link-receptor pair was estimated as the product of the link's  
776 emission rate for that hour and  $C_x$ , using the link's closest distance to the receptor (precomputed to save  
777 time). Only if the potential impact exceeded  $1.5 \times 10^{-5}$  of the maximum possible concentration was that  
778 link-receptor pair and hour calculated. Thus, only those link-receptor pairs and hours that can contribute  
779 at least  $1.5 \times 10^{-5}$  of the maximum concentration that can result from a high volume link are selected; low  
780 traffic and/or distant links are screened out. This algorithm slightly decreases concentrations at locations  
781 distant from large roads, but no significant changes are seen for receptors near larger roads. The  $1.5 \times 10^{-5}$   
782 threshold, AADT=100,000, and  $x=25$  m parameters are empirically determined values; smaller values  
783 increase computation time but lead to more accurate results.

784 The above steps dramatically increased computational speed and obtained results that were nearly  
785 identical to those using all source-receptor pairs and the numerical algorithm. Still, computation of  
786 annual averages for the largest receptor network required several days on a workstation.

#### 787 **9.5 Interpolation concentrations and estimating errors**

788 As noted in the text, concentrations were estimated from concentrations predicted at receptors using two  
789 interpolation methods. The first uses the "nearest neighbor" (NN) technique and estimates the unknown  
790 as the concentration at the nearest receptor. Errors were calculated as the absolute difference in  
791 concentrations between all pairs of receptor separated by distance  $\Delta x$ :

792 
$$\Delta C_{NN, i, \Delta x} = | C_i - C_{i+\Delta x} | \quad (5)$$

793 where  $C_i$  and  $C_{i+\Delta x}$  = known concentrations at receptor  $i$  and a second receptor displaced in either E or N  
 794 direction by  $\Delta x$ . The second interpolation method is equivalent to an inverse-distance-weighted (IDW)  
 795 average, and the unknown concentration is estimated as average of concentrations at the four nearest  
 796 receptors:

797 
$$\Delta C_{ID, i, \Delta x} = | C_i - (C_{i+\Delta x} + C_{i-\Delta x} + C_{i+\Delta y} + C_{i-\Delta y})/4 | \quad (6)$$

798 where  $\Delta x$  and  $\Delta y$ =equal separation distances in E and W directions, respectively.

799 Concentration errors were expressed as absolute concentration differences, as given by eqs. (5) and (6),  
 800 and by the relative absolute concentration differences (R $\Delta C$ , %) by dividing by the average concentration:

801 
$$R\Delta C_{NN, i, \Delta x} = 100\% \Delta C_{NN, i, \Delta x} / [(C_i + C_{i+\Delta x}) / 2] \quad (7)$$

802 
$$R\Delta C_{ID, i, \Delta x} = 100\% \Delta C_{ID, i, \Delta x} / [C_i / 2 + (C_{i+\Delta x} + C_{i-\Delta x} + C_{i+\Delta y} + C_{i-\Delta y})/8] \quad (8)$$

803 The R $\Delta C$  is equivalent to the absolute fractional bias. At finer spatial resolutions, i.e., as  $\Delta x \rightarrow 0$ , both  
 804 error metrics approach 0.

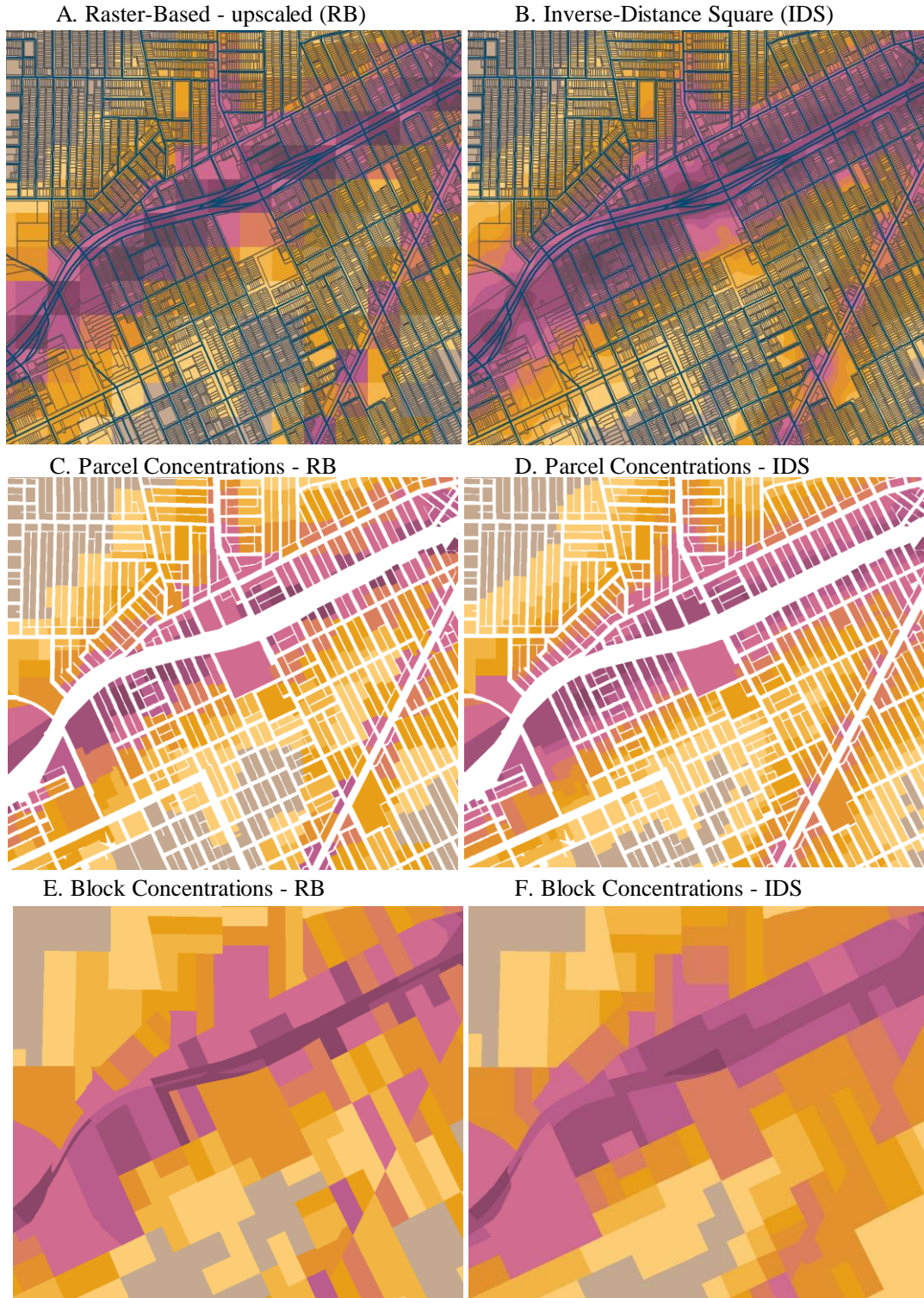
805

806

807

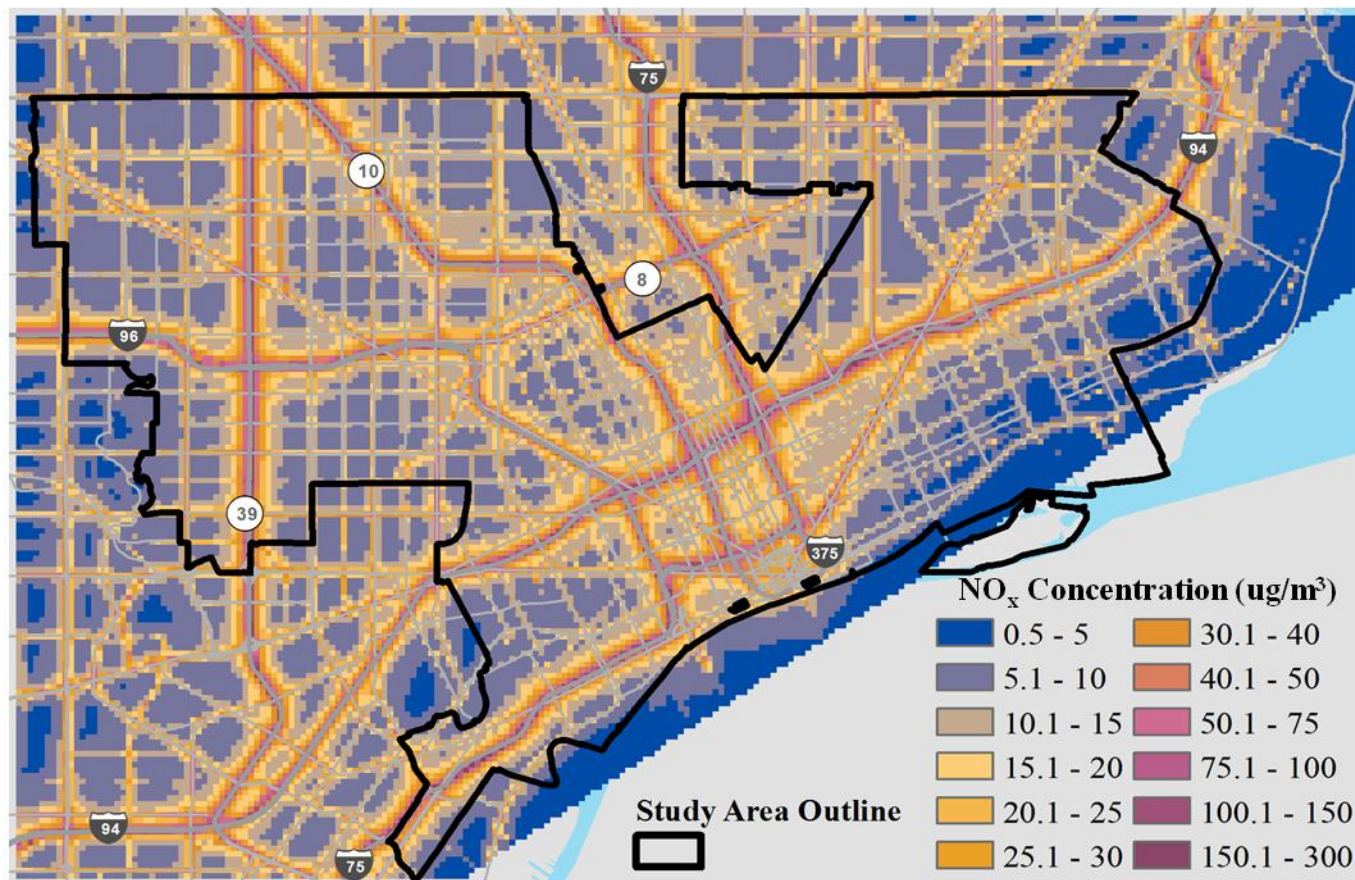


808 **Supplemental Figure 1.** Comparison of up-scaled raster-based (RB) and inverse-distance squared  
 809 weighting (IDS) joining schemes for parcel- and block-level concentrations. Top figure shows underlying  
 810 raster, roads, and parcel and block boundaries. Middle figures show estimated parcel-level  
 811 concentrations. Bottom figures show estimated block-level concentrations.



Region is 1.2 x 1.4 km along I94  
 Shading shows NO<sub>x</sub> concentrations  
 Gray lines show property parcels  
 Purple lines show census blocks

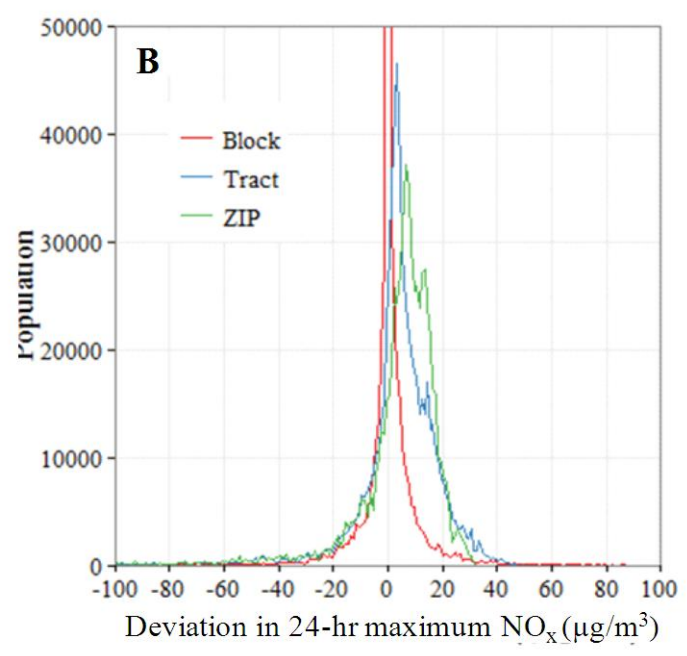
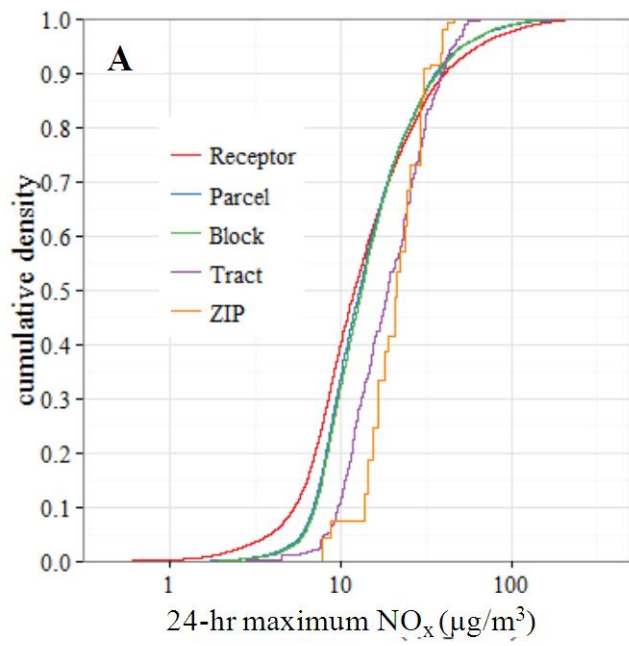
813 **Supplemental Figure 2.** Modeled maximum 24-hr NO<sub>x</sub> concentrations (μg/m<sup>3</sup>) over study region using  
814 receptors on 150 m centers. The area for which data were analyzed is shown with a black outline.



815

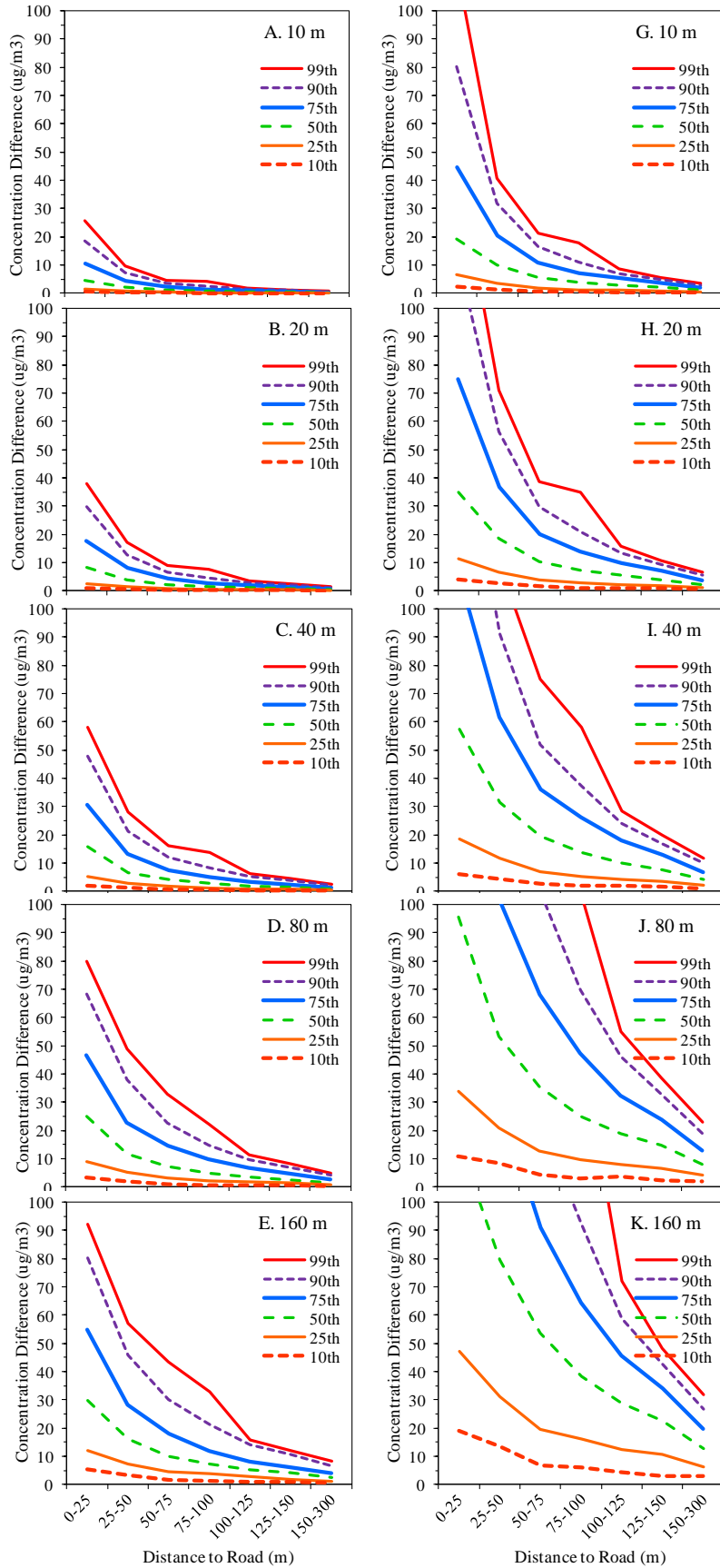
816 **Supplemental Figure 3.** Comparison of NO<sub>x</sub> concentration estimates for several geographic zones. A:  
817 Distribution of maximum 24-hour NO<sub>x</sub> concentrations in Detroit at receptors and four geographic zones  
818 (not weighted by population). B: Distribution of concentration deviations for three zones (from parcel  
819 concentrations). Figure B is truncated at 100 μg/m<sup>3</sup>, thus the most elevated concentrations are not shown.





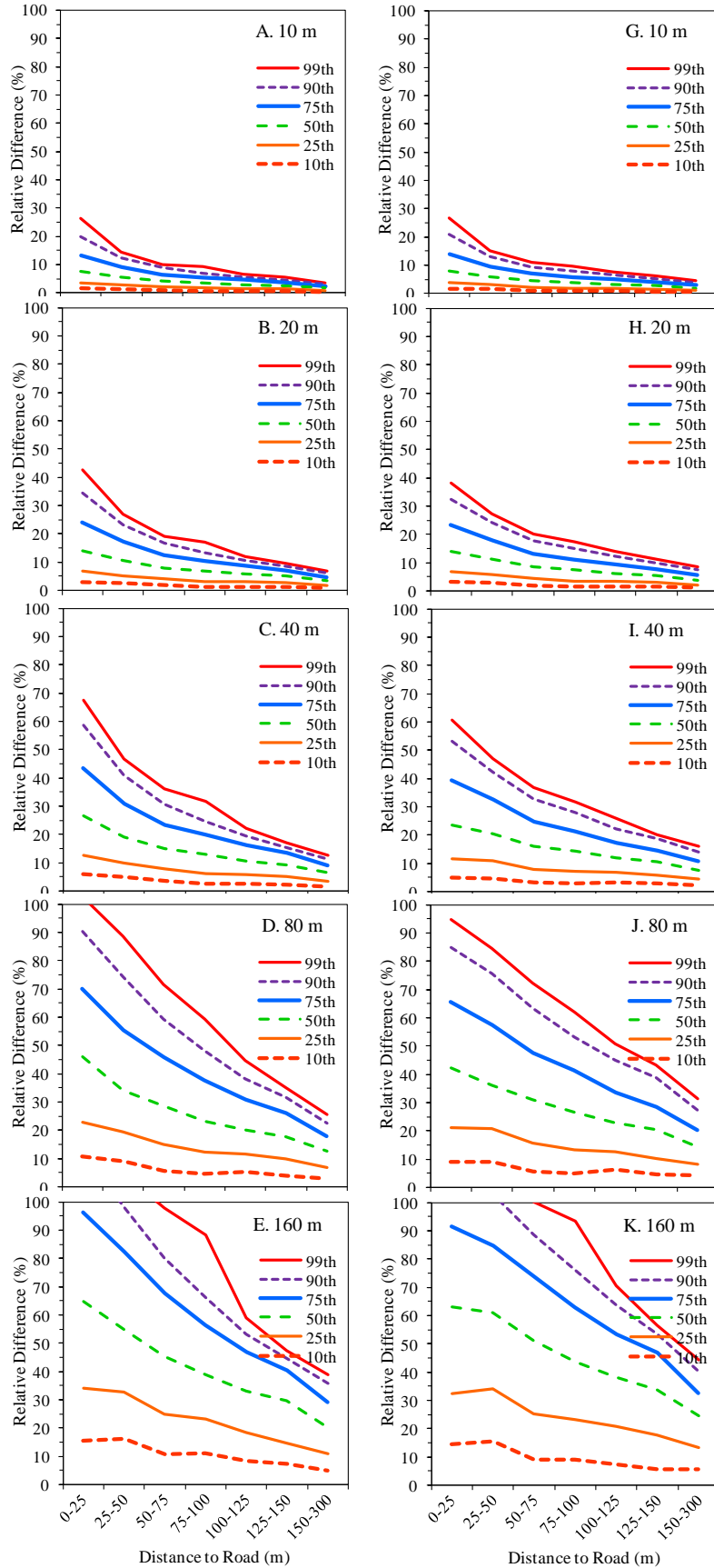
820  
821

Supplemental Figure 4. Absolute concentration differences grouped by distance to roads for estimate of 10, 20, 40, 80 and 160 m distance. Left: monthly average; Right: 98<sup>th</sup> percentile 1-hr average.





Supplemental Figure 5. Relative concentration differences grouped by distance to roads for estimates of 10, 20, 40, 80 and 160 m from known values. Left: monthly average; Right: 98<sup>th</sup> percentile 1-hr average.



828  
 829  
 830  
 831  
 832  
 833  
 834

**Supplemental Table 1.** Population-weighted concentration deviations (1) and absolute concentration deviations (2) for maximum 24-hr NO<sub>x</sub> concentration (µg/m<sup>3</sup>). R denotes linear correlation with parcel level data; F2 is factor of two agreement; n=sample size. Deviations are defined as the difference between concentrations estimated for individuals within the zone compared to that at the parcel level. Note that at tract and ZIP-code levels, the 75th percentile concentration deviation exceeds the median concentration (shown in Table 1), indicating large exposure errors for at least 25% of the population.

Statistic	Concentration Deviations (1)			Absolute Concen.Deviations (2)		
	Block	Tract	ZIP	Block	Tract	ZIP
Mean	0.1	3.4	3.7	4.2	11.1	12.0
Std. Dev	11.3	17.7	18.2	10.5	14.2	14.2
Min	-260.3	-263.5	-278.3	0.0	0.0	0.0
10th	-4.8	-9.9	-11.1	0.0	1.3	2.1
25th	-0.4	-0.3	0.6	0.0	3.2	4.9
50th	0.0	4.2	6.9	0.6	7.1	9.2
75th	1.0	11.5	12.8	4.1	14.6	14.8
90th	6.0	19.2	17.4	11.2	23.5	20.9
99th	30.5	34.5	26.9	46.6	69.6	72.8
Max	238.7	51.8	35.2	260.3	263.5	278.3
R	-	-	-	-	-	-
F2	0.006	0.168	0.182	-	-	-
N	357,962	357,962	357,962	357,962	357,962	357,962

835